Article

JFPE

Journal of Fire Protection Engineering
0(00) 1–26

DOI: 10.1177/1042391512459640
jfe.sagepub.com

SAGE

Numerical investigation of fires in small rail car compartments

X Hu
Fire Safety Engineering Group, the University of Greenwich, Greenwich, London

Z Wang
Fire Safety Engineering Group, the University of Greenwich, Greenwich, London

F Jia
Fire Safety Engineering Group, the University of Greenwich, Greenwich, London

ER Galea
Fire Safety Engineering Group, the University of Greenwich, Greenwich, London

Abstract

In this article, an enhanced flame spread model is used to simulate a rail car compartment fire test. The model was found to be able to reproduce the following experiential results: the predicted progressive burning locations are consistent with the experimental record; the predicted temperatures and heat fluxes at various locations essentially follow the measured trends; and the predicted onset of flashover is within 9% of the measured time of 180 s. The sensitivity of the predicted time to flashover is assessed using 18 fire scenarios in which the uncertainties in the measured material properties are systematically examined. The time to flashover is found to be most sensitive to changes in seat material properties. For the investigated rail car compartment, the impact of porosity of the overhead luggage rack structure on time to flashover is also examined and found to be significant for small ignition source fires.

Keywords

Train fire safety, ignition temperature, flame spread rate, time to flashover

Corresponding author:
Edwin Galea, the University of Greenwich, 30 Park Row, Greenwich, London SE10 9LS, UK.
Email: e.r.galea@gre.ac.uk

Introduction

Flashover is a critical point in rail car fire development at which the fire grows rapidly to engulf the entire car in a very short period of time. The time to flashover is generally considered to mark the end of the survivability period for those passengers still within the car. Small passenger compartments have often been used in rail cars such as the BF4 car built in 1985–1986 [1]. The relative small volume of rail car compartments can result in flashover occurring sooner than in a large uncompartmented rail car constructed from the same materials. Flashover within a compartment not only creates non-survivable conditions but also poses a high risk of spread of the fire to other areas of the rail car.

Great efforts have been made to improve passenger train fire safety by railroad administrations worldwide. For example in 1984, a fire safety guideline for passenger rail cars was proposed by the Federal Railroad Administration (FRA) in the USA and has been revised several times, as reviewed in [2,3]. One of the major objectives of train fire safety design is to prevent an interior fire within a rail car that results in the onset of non-survivable conditions. Properties of passenger rail car interior materials are regarded as a key factor in determining appropriate fire safety requirements. For a given fire, as a rail car compartment is more prone to the occurrence of flashover than a large rail car, materials used in such compartments become even more important in terms of fire safety than materials used in other areas.

Full-scale mock-up fire tests are an important means of investigating fire behavior of passenger train materials. Experimental fire data can be used to evaluate if these interior materials reach an acceptable fire performance by simply estimating the time to flashover or analyzing the likely impacts of fire hazards on the evacuating passengers. Six large-scale railcar fire tests conducted in tunnels with varied types of vehicles have been reviewed by Ingason [4]. Some fully-furnished rail car fire tests have been conducted recently, for example, a test conducted in an Amtrak coach rail car [3], a test conducted in a suburban rail carriage [5] and a test within a compartment of a BF4 rail car [1]. Although full-scale tests can provide reliable fire assessments, the high costs of conducting such tests limit their use in fire investigation. Fire behavior is dependent on both the configuration of the car including ventilation and the nature of the interior materials. It would be prohibitively expensive to investigate with full-scale experiments a large number of car configurations and various combinations of interior materials. Therefore, alternative fire safety assessment methods with lower costs are desirable. Compared with real fire tests, fire field modeling, which can provide more detailed information on fire development, is much more cost effective. Numerical simulations can be set up with relative ease and run for different fire scenarios with changes of the environmental conditions to understand how parameters relating to compartment configurations and interior material properties affect the fire development.

In this study, the fire field modeling tool SMARTFIRE [6] is used to simulate the rail car compartment fire test in [1]. Simulations are performed using a flame spread model [7] incorporating multiple ignition criteria, rather than using the

single criterion of surface ignition temperature. The fire model is described in the next section. In the Simulation and Results section, the full-scale rail car compartment fire test is described, followed by detailed simulation results and analysis. Variations in the predicted time to flashover caused by the uncertainty of the measured material properties are also investigated in this section. In order to investigate the effect of rack configuration, fire scenarios with variations in porosity of the luggage rack structure, with or without luggage and with different ignition sources, are numerically simulated in the section before Conclusions.

Fire-field model

In field modeling, the fluid is governed by a set of three-dimensional partial differential equations. The generalized governing equation for all variables is expressed in the form of equation (1)

$$\frac{\partial \rho \Phi}{\partial t} + div(\rho \vec{U} \Phi) = div(\Gamma_\Phi \nabla \Phi) + S_\Phi \tag{1}$$

where Φ represents the fluid variable; ρ and $\vec{U}$ are the local density and velocity vector; Γ_Φ is the effective exchange coefficient of Φ; S_Φ represents the source term for the corresponding variable Φ and time t is an independent variable.

The SMARTFIRE V4.1 [6] software used to perform the fire simulations in this study has been described in previous publications [6–10] and so only a brief outline is presented here. The computational fluid dynamics (CFD) engine in SMARTFIRE has many physics features that are required for fire field modeling [11,12]. Details of the common sub-models used in CFD fire simulations, such as the multiple ray radiation model, the volumetric heat release model, the gaseous combustion model (utilizing an eddy dissipation model (EDM) [13]), the smoke model and the k-epsilon turbulence model can be found in [12]. In the simulations presented here, the EDM is used to simulate the burning of the combustible gases released from the ignited materials. The multi-ray radiation model with 48 rays is used to represent thermal radiation.

The flame spread model used in these simulations was initially developed in [7]. The approach has been further validated by successfully reproducing a post-crash aircraft fire test [8] and the Station Nightclub fire reconstruction [9]. It has also been used to investigate the impact of a post-crash cabin fire on passengers evacuating a large aircraft [10]. In this model, 1D heat conduction is solved along the thickness of the material modeled. The heat flux at the top surface, the face exposed to the fire, is the sum of convective and radiative heat fluxes. The bottom surface can be assumed to experience no heat loss or alternatively to be at ambient temperature. In the simulations performed in this study, the bottom surface is assumed to be at ambient temperature. Furthermore, no surface deformation and reduction of the material thickness due to burning is assumed. All combustible surfaces are assigned a face patch which identifies them as a burnable material. Each face patch is labeled with a unique patch number which defines their location and material

properties. At the end of each time step, conditions at a cell face of a burnable face patch are assessed to determine whether ignition conditions are reached. The ignition of the interior materials is determined by one of the following ignition criteria:

a. The material surface temperature reaches its ignition temperature; or,
b. The pyrolysis front advances from an adjacent burning cell face to the cell face in question, determined from a measured flame spread rate.

Without the ignition criterion (b), the current flame spread model is identical to the Fire Dynamics Simulator (FDS) flame spread model which uses the heat release rate per unit area (HRRPUA) approach [14]. The flame spread rate in this enhanced flame spread model is the only additional parameter. In theory, the criterion of surface ignition temperature alone is sufficient for the simulation of flame spread along combustible solid surfaces. In practice however, within CFD fire simulations, ignition of a solid surface can be strongly mesh dependent and as fire is a complicated and large-scale phenomenon it would be extremely difficult, if not impossible, to eliminate this reliance altogether from simulations of flame spread over solid surfaces. In the case of wind opposed flame spread, extremely fine meshes in areas of flame fronts are required to predict flame spread accurately. It is very likely that with a coarse mesh, no flame spread would be predicted at all. But as practical fire simulation is normally concerned with large-scale phenomena, it can be prohibitively expensive and impractical to use extremely fine meshes in such simulations. In addition to this dilemma, it is impossible to know in advance, at the mesh generation stage, what fire conditions (wind assisted or opposed) are likely to occur at any given point. A practical engineering method to overcome these difficulties is to introduce a flame spread rate, which is measurable from fire tests, alongside surface ignition temperature in the enhanced flame spread model used in this analysis.

Of the two ignition criteria used in the current flame spread model, criterion (a) is the dominant one once the fire is sufficiently large to be self-sustaining. The effect of criterion (b) is significant only in the very early stage of fire development when the fire is weak and the dominant modes of heat transfer for flame spread are convection from the flame to the solid surface and conduction within the solid. Due to the coarse mesh used in large scale fire simulations, these heat transfer modes cannot be predicted with adequate accuracy to result in self-sustained flame spread over the solid surface. One option to overcome this problem was proposed in [15] in which an artificially large heat release rate (HRR) of $1500\,kW/m^2$ was employed in the simulation of the Station Nightclub fire as an ignition source, in order to create self-sustained flame spread. In the current study, the alternative approach is taken of using ignition criterion (b), instead of an unrealistically large ignition source. The role of criterion (b) is to maintain flame spread at the early stage of fire growth. Once flame spread over the solid surface is self-sustaining, the contribution of this criterion to the prediction of flame spread is negligible.

If one of these two ignition criteria is reached, a cell face begins to burn. Once a cell face is ignited, it starts to release a certain amount of fuel according to the time-dependent burning rate (kg/m^2s) or HRR for this material. Besides the ignition temperature and flame spread rate, a number of other material properties for the solid surface are also required. Model input parameters are as follows:

- Surface ignition temperature (°C);
- Upward, lateral and downward flame spread rates (m/s);
- Thickness (m);
- Density (kg/m^3);
- HRR per unit area (kW/m^2);
- Specific heat (J/kg);
- Thermal conductivity (W/mK);

The surface ignition temperature can be derived from the measured time to ignition from cone calorimeter tests [16]. Ignition temperatures for some common solid materials can be found in [17]. The HRR for surface materials under various external heat fluxes can be obtained from small-scale tests such as cone calorimeter tests.

The flame spread rate required in the model is the velocity of the pyrolysis front moving over the solid surface. This velocity, for solids behaving as thermally thick, is a function of the external heat flux to the solid surface, the ignition temperature and the thermal inertia of the solid [16,17]. As reviewed in the study of flame spread rate for polyurethane (PUR) foam in [15], the lateral flame spread rate can be measured using small-scale apparatus such as LIFT.

In order to minimize the mesh dependence of numerical predictions of flame spread over solid burnable surfaces, the model in this study is further refined by dividing each solid surface cell, called the 'original face cell', into a number of sub-cells. The ignition criterion (b), which was applied to the 'original face cell', is also adopted for each sub-cell here. Once a sub-cell face is ignited, it starts to release a certain amount of fuel according to its area. The fuel released from this sub-cell contributes to the control volume adjacent to the 'original face cell'. The current implementation method for the flame spread model thus utilizes a very fine equivalent mesh for flame to spread based on the flame spread rate input without any increase in the number of control volumes in the computational domain. The additional computational cost due to refining the surface cells is negligible compared with the typical CFD runtime requirements. This modification allows flame spread along the surface to progress in a smooth manner if the number of sub-cells is adequate and is less sensitive to the fineness of the mesh in the gas phase.

Combustion of the gaseous fuel generated from the burning of the solid fuel is modeled with the EDM. In non-premixed turbulent fires, the fuel and oxidant are in separate eddies. The combustion process is usually much faster

than the eddy mixing process. Therefore, the combustion rate can be determined by the rate of intermixing of fuel and oxygen eddies. EDM is just such a model, as proposed by Magnussen and Hjertager [13], in which the fuel-burning rate is given by

$$R_f = A\rho\frac{\varepsilon}{\kappa}\min\left\{Y_{\mathrm{f}}, \frac{Y_o}{r}, B\frac{Y_p}{1+r}\right\} \tag{2}$$

where the model constants A and B usually take the values of 4.0 and 1.0, respectively, ρ is the density, k and ε are the turbulent kinetic energy and the turbulent dissipation rate, respectively, r is the stoichiometric mass ratio of oxidant (air) to fuel. As fast and complete combustion is assumed in the model, gas temperatures can be over-predicted, but this is dependent on the mesh used, boundary conditions applied and the calculation accuracy of radiant energy exchange, all of which can influence the prediction of gas temperature.

Simulations and results

Fire experiment

The SP Technical Research Institute of Sweden conducted a fire test within a train compartment in 2009 [1]. The compartment with a size of 1.96 m × 2.00 m × 2.40 m was equipped with furniture as seen in Figure 1. The open doorway of the compartment is 2 m high. There were a total of six seats in two rows in the compartment. The seat consisted of fabric on PUR foam upholstery. Figure 1(b) shows the two connected seats (Seat 1 and Seat 2) in each seat row while the third seat (Seat 3) in each row was separated by a table. Metal laminate panels covered the two short walls and high pressure laminate (HPL) panels covered the two long walls. The metal laminate wall panel consisted of 1.6 mm metal laminate glued onto 18 mm plywood. HPL laminate wall panel consisted of 1 mm HPL laminate glued onto 18 mm plywood. The wood table was 30 mm thick. The floor was covered with a polyvinyl chloride (PVC) carpet. The fire was initiated by igniting a seat with a 7 kW propane burner, which was located at 10 mm from the backrest and 10 mm above the seat at one of the rear corners. The square burner had a side length of 115 mm. The flame from the burner had been applied to the seat for 76 s.

In order to characterize the fire as precisely as possible, the compartment was heavily equipped with detectors. Three thermocouple trees and two radiation detectors were placed as shown in Figure 1(b). The radiation detector 1 was facing seat 2 and detector 2 was facing upwards. The heat release rate was measured using the setup of the ISO 9705 test standard. More details about the test can be found in the SP report [1].

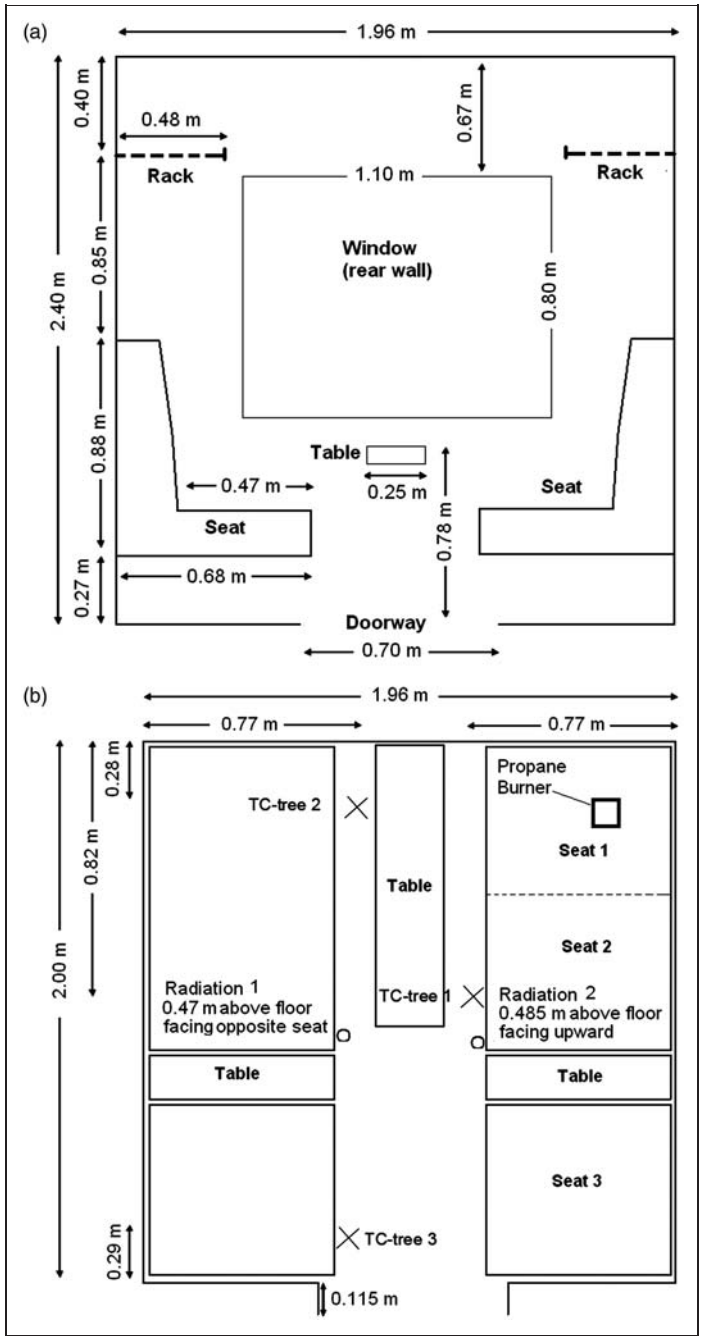

Figure 1. (a) Schematics of investigated rail car compartment, (a) side view and (b) floor plan.

Simulation description

An unstructured mesh is used to represent the complex rail car compartment geometry as shown in Figure 2. As was the case in the real fire test, the seats, walls, floor and wood tables are set in the model as combustible while the window and ceiling are non-combustible. The fire properties of combustible materials except those of luggage racks, including the thickness, density, heat release rate, ignition temperature, thermal conductivity, specific heat and heat of combustion, were taken from the experimental report [1]. As the major part of the luggage racks consisted of wood, the material properties for the wood table are used for the racks, the same

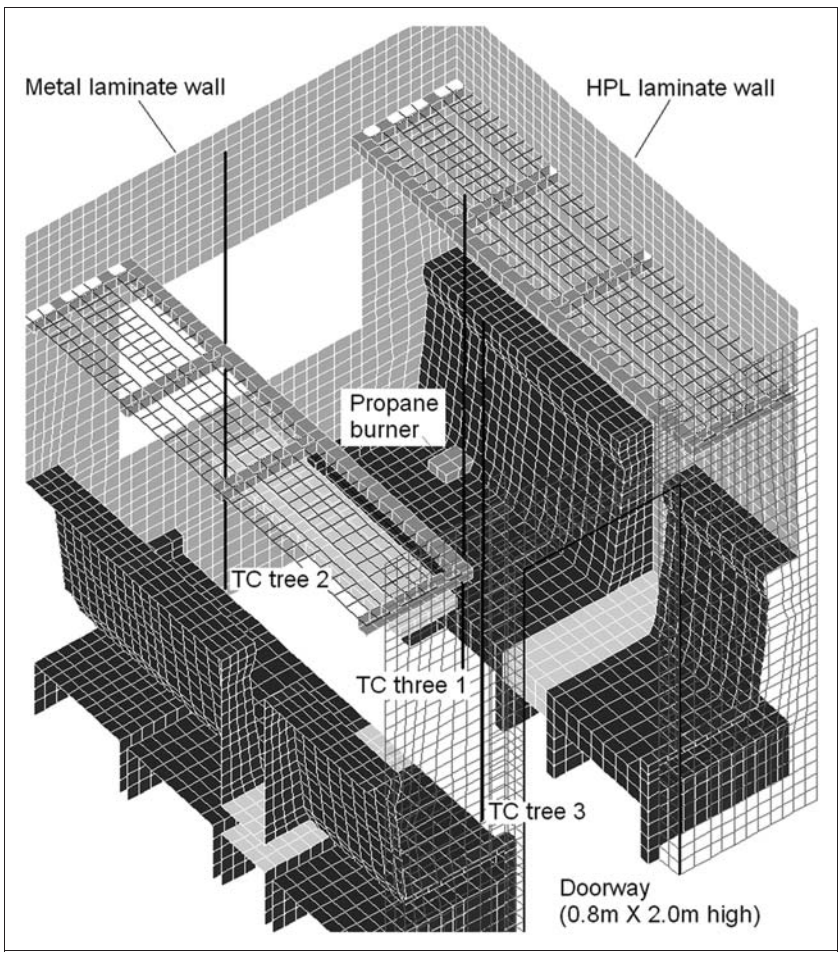

Figure 2. Representation of the fire compartment in the simulation.

approach taken in [1]. The openings within the rack structure, which yield an estimated porosity of 30%, are also represented in the model (see Figure 1(a)).

All material properties for the model inputs are the same as those used in the simulations reported in [1] except the flame spread rate (see Table 1). HRRs under various levels of radiance were obtained from tests with the cone calorimeter, ISO 5660-1. The ignition temperature and thermal inertia were evaluated from the time to ignite the specimen in the cone calorimeter as a function of radiance level. The density of a material was derived from its measured weight and volume. The specific heat was selected from publications by the authors of [1]. The thermal conductivity was extracted from the thermal inertia.

It is noted that ignition temperatures for the two wall panels, metal laminate and HPL laminate are much higher than those for other materials. The high ignition temperatures are a direct result of the difficulties in igniting these materials in the cone calorimeter tests. Unlike other materials with relatively low minimum radiation flux for ignition, the metal laminate was only ignited under radiation fluxes of 50 kW/m^2 or more in the cone calorimeter tests and the radiation flux to ignite the HPL laminate wall panel was at least 35 kW/m^2.

Flame spread rates were not provided in the experimental report [1]. However, the fire behavior of the double seat was investigated twice, once during free-burning in the furniture calorimeter and once burning inside the ISO 9705 room. It was shown that there is no significant difference in fire dynamics depending on whether the seat was free-burning in the furniture calorimeter or placed in the ISO 9705 room. From the images of the test inside the ISO 9705 room, it is observed that the flame spread from the seat base to the seat backrest at a height of approximately 0.2 m at 54 s and to the top of the seat backrest (approximately 0.7 m from the base) at 132 s. It took approximately 125 s for the flame to spread from the seat base to the top of the seat backrest in the free burning test. It was reported that the fire on the ignited seat developed faster in the full-scale test than in the free-burning

Table 1. Material properties [1]

		Seat	Metal laminate	HPL Laminate	PVC carpet	Table
Thickness (m)		0.05	0.02	0.02	0.002	0.03
Density (kg/m^3)		77	648	548	1400	616
Conductivity (W/mK)		0.015	1.07	0.11	0.25	0.11
Specific Heat (J/kg)		1200	2500	2500	1500	2500
Ignition temperature (°C)		346	607	526	278	433
Flame spread rate (m/s)	Upward	0.005	0.001	0.001	0.001	0.001
	Lateral	0.0025	0.001	0.001	0.001	0.001
	downward	0.001	0.001	0.001	0.001	0.001

fire test. From this information, it is estimated that an average upward flame spread rate is no less than 0.005 m/s for the seat. The difference in the lateral flame spread rate between the two tests appears to be significant, with an estimated flame spread rate of 0.0025 m/s being derived from the test inside the ISO 9705 room. As the simulation presented in this article relates to an enclosure fire, the lateral rate derived from the ISO 9705 room is used. The downward flame spread rate is assumed to be 0.001 m/s.

The flame spread rates for other materials cannot be estimated from the tests reported in [1] as no burning test similar to the seat testing was conducted for them. Considering the fact that the fire was well established after the seats were in flame, the ignition of other materials is expected to be predominantly caused by ignition criterion (a), i.e. the surface ignition temperature. Therefore, the lack of flame spread rates for other materials does not significantly affect the simulation of the rail car compartment fire. However, as a model parameter, 0.001 m/s, which is much lower than the lateral flame spread rate for most solid materials in the LIFT test [18], is assigned for materials other than the seat. A material with an assigned flame spread rate of 0.001 m/s indicates that ignition is solely controlled by the surface temperature criterion. Wall emissivity is assumed to be 0.8 for all surface materials.

As reviewed in [1], the heat flux received by the seats is around 35 kW/m^2 in the test fires and for the other materials, heat fluxes are around 50 kW/m^2. Therefore, cone calorimeter HRR data for these materials under corresponding heat fluxes is likely to be representative of their burning behavior in the rail car test fires. Presented in Figure 3 are the HRR curves extracted from the cone calorimeter

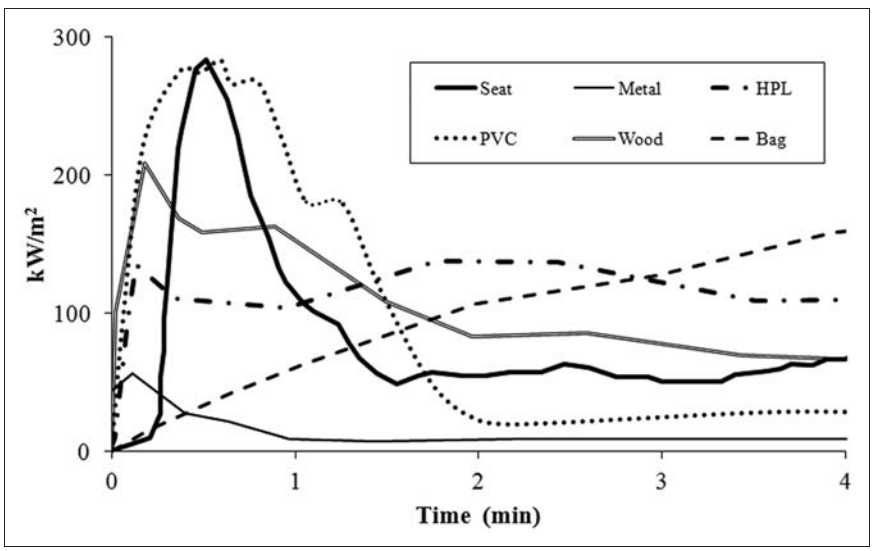

Figure 3. Heat release rate (HRR) data for interior materials.

test data in [1] except for bag, which is introduced in the rack structure section later. These HRRs are assigned to the rail car interior materials in the simulations.

The EDM [13] is used to simulate the burning of the combustible gases released from the ignited materials. The main fire load in the test was the seats containing PUR foam. For this reason, the gas phase reaction is specified to be the combustion of PUR (this is the same assumption that was made in [1]). An average effective heat of combustion of 17.5 MJ/kg is taken for PUR foam ($C_1H_{1.7}O_{0.3}N_{0.07}$) [19]. The multi-ray radiation model with 48 rays is used to represent thermal radiation. The duration of the fire was approximately 250 s and simulations are carried out with a time step size of 1 s.

Mesh quality is always crucial to the success of any CFD fire simulation. In these simulations, the computational domain is extended by 2 m to include a region outside the fire compartment in order to correctly model the flow through the open door. To examine the grid size dependency, two different mesh budgets with 69,732 cells and 310,928 cells, respectively, were investigated. The cell size is about 0.06 m at locations near the initially ignited seat for the coarse mesh and it is approximately 0.03 m for the fine mesh. Presented in Figure 4 are the predicted HRRs (Figure 4(a)) and temperatures at 2.3 m above the floor for thermocouple tree 1 (Figure 4(b)). The predicted HRRs with the two different mesh scenarios are almost identical before 130 s and a time separation of around 10 s only exists between the rising HRR profiles after 170 s (Figure 4(a)). The predicted temperature curves at 2.3 m above the floor of thermocouple tree 1 from the two mesh scenarios are also quite similar (Figure 4(b)). These results suggest that the difference in predictions between the two mesh scenarios has no significant bearing on the essential trends of the predicted spread of flame inside the rail car. Thus, it was concluded that the relatively coarse mesh consisting of 69,732 cells was appropriate for the simulation of the rail car fire. It was noted that the computational cost for the fine mesh (99 h) is significantly higher than for the coarse mesh (only 19 h). As more than forty scenarios are investigated in this study, only the results from the coarse mesh will be considered for the remaining material sensitivity studies.

Simulation results

Firstly, the measured and predicted heat release rates are compared in Figure 5. Due to saturation of the gas analyzer for heat release rates above 1800 kW, no HRR data were obtained using oxygen depletion calorimetry after 180 s. The HRRs after 180 s are an estimation based on temperature measurements in the exhaust gases [1]. In Figure 5, the solid squares represent the measured data before 180 s while the open squares are estimations after this time. The measured HRRs are below 35 kW in the first 90 s, followed by a gradual increase. It reaches a value of 1050 kW at 175 s. Then the estimated HRR rapidly increases and reaches an estimated peak value of 4520 kW. The predicted HRRs essentially follow the measured trends and are in good agreement with the measured data before 200 s. However, unlike the continuous increase of the HRR in the experiment, the

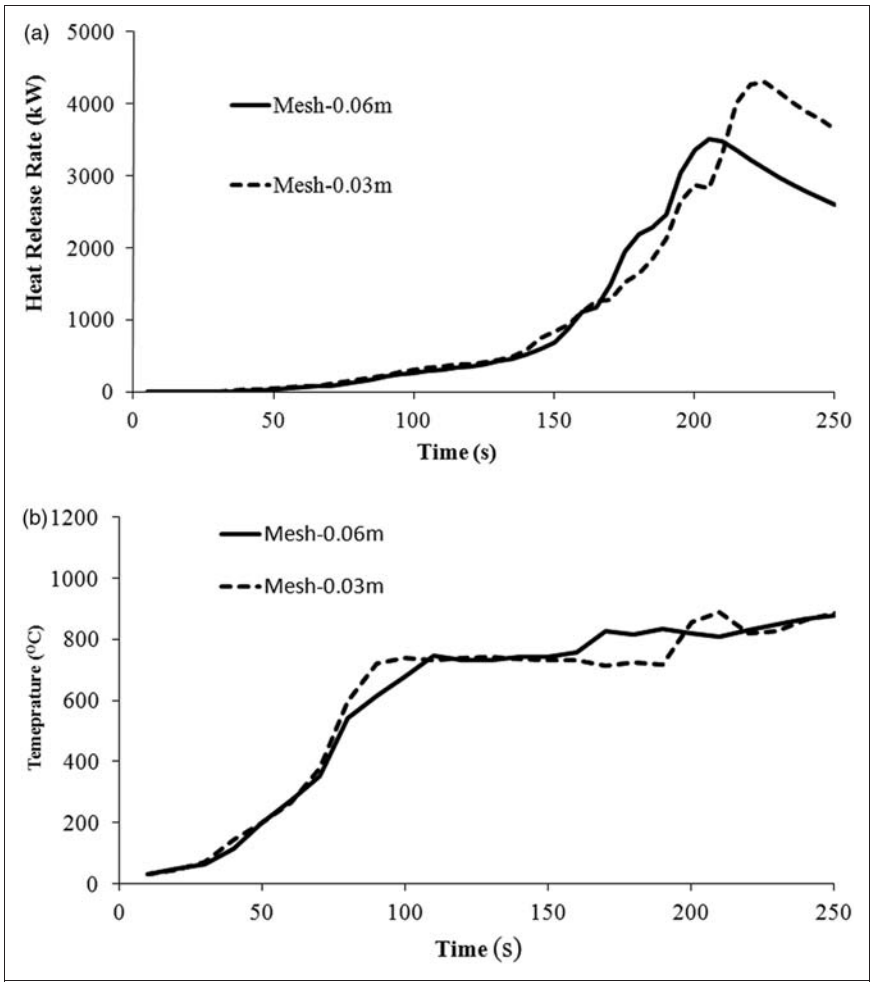

Figure 4. Predicted heat release rate (HRR) (a) and temperature at 2.3 m above the floor for thermocouple tree 1 (b) for two different computational meshes.

predictions start to decrease after 200 s. However, the reported HRRs after 180 s may be subject to uncertainties as they were estimated from temperature measurements in the exhaust gases.

The definition of flashover for enclosure fires is generally accepted as occurring when the upper layer gas temperature exceeds 600°C [20,21]. In the experimental analysis [1], the onset of flashover was defined as occurring when the HRR begins to rapidly escalate. For the purpose of convenient comparisons among all the design scenarios considered in this study, the measured HRR value of 1.17 MW at the reported onset of time to flashover (180 s) is regarded as a criterion for flashover in this study. With this criterion, the predicted time to flashover is

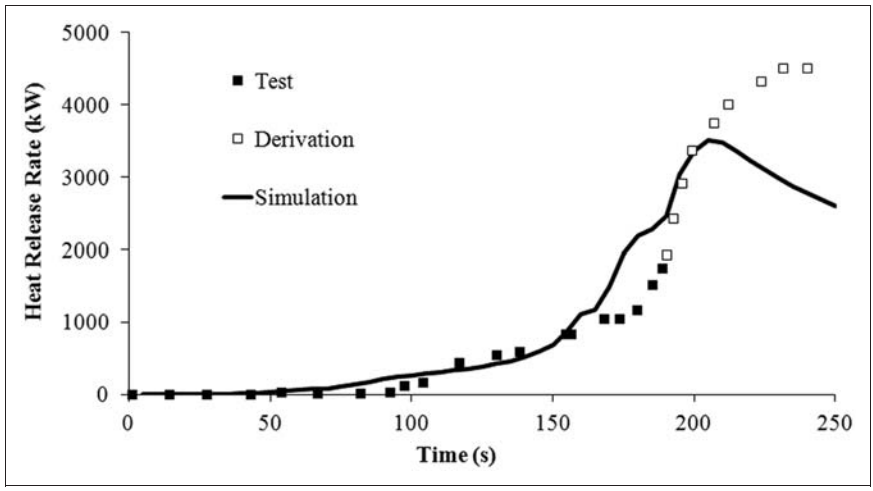

Figure 5. Measured and predicted heat release rate (HRRs).

Table 2. Comparision of fire development between observation and model prediction (See Figure 1(b) for seat locations)

Time (s)	Experimental observation [1]	Model prediction
60	Entire back of Seat 1 was in flames	Whole base and most of the back of Seat 1 is ignited (Figure 6(a))
90	The luggage rack above Seat 1 was in flames	Half of the rack and the most of the side wall above the rack is ignited (Figure 6(b))
150	Entire Seat 2 was ignited	All of Seat 2 and upper half of the side wall are ignited; the top of seat back of Seat 3 is also ignited (Figure 6(c))
180	Seat 3 and the entire left seat row were ignited	All seats, side walls and carpet are ignited (Figure 6(d))

around 165 s (Figure 5), which is only 15 s sooner than the time observed in the fire test, with an error of less than 9%.

Secondly, some important events observed during the test [1] are compared with the model predictions of burning positions at these same times (see Table 2). As can be seen from Table 2, the key observations in the numerical predictions match those noted in the experiment.

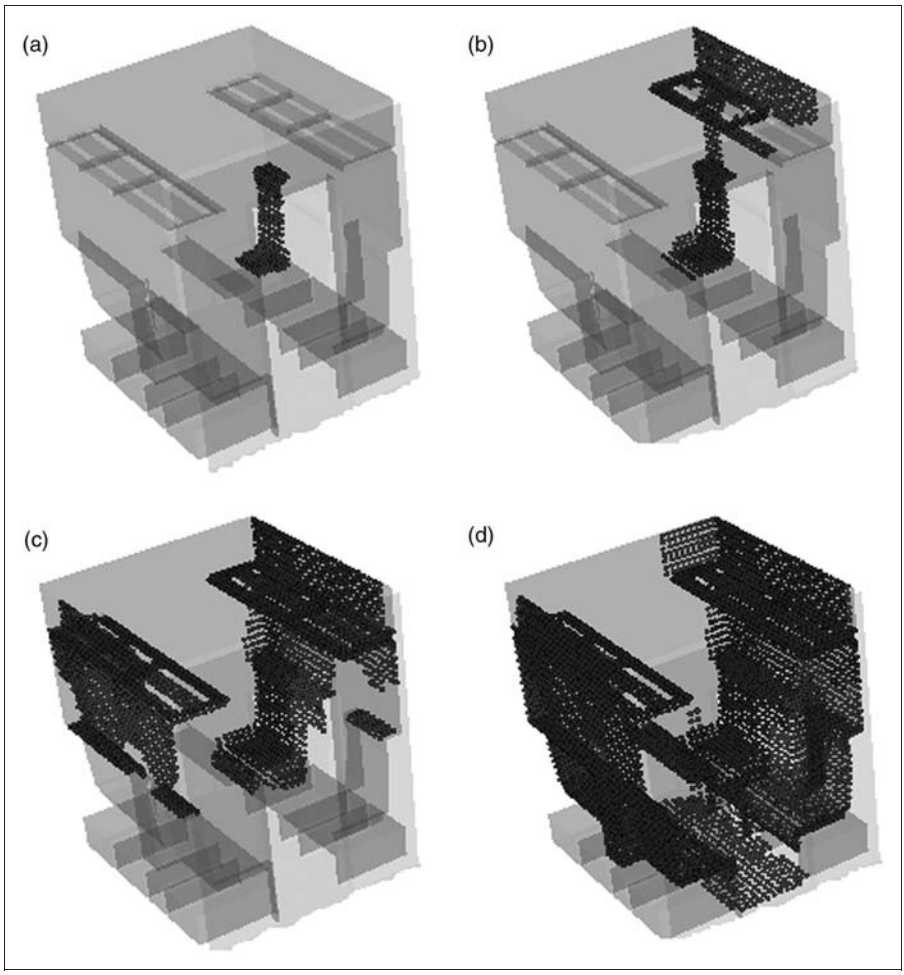

Figure 6. Predicted cell face burning locations at (a) 60 s, (b) 90 s, (c) 150 s and (d) 180 s.

Related to these observations are the predicted locations of the cell faces that have been ignited at the four key times as shown in Figure 6. At 60 s, the entire back of the seat where the fire was initiated (Seat 1) was covered by flame in the test. As seen in Figure 6(a), at this time, the whole base and most of the seat back are ignited in the simulation.

At 90 s, the luggage rack above the seat of fire origin was observed to be burning in the test. Similarly, one half of the rack is burning in the simulation. It is also noticed that the part of wall above this rack is predicted to be burning. The entire seat immediately adjacent to the seat of fire origin (Seat 2) was in flames at 150 s in the test and it is also fully ignited in the simulation. In addition, in the simulation the upper part of the left side wall and the left rack are involved in the fire at this

moment. However, there are no experimental data as to when the left side wall starts to burn. The lack of this information may be the result of poor visibility due to heavy smoke in the upper layer. At 180 s, flashover occurred and the seats on the left seat row (opposite the seat of fire origin) were ignited in the test. Due to the slightly earlier occurrence of the predicted flashover (165 s), most of the interior materials, including the carpet, are ignited at 180 s in the simulation. From these observations it is concluded that the fire model is capable of reproducing the major events observed during the fire test to a reasonable degree of accuracy.

Thirdly, the measured and predicted temperatures at 2.3 m and 1.0 m above the floor at the three thermocouple trees are compared and shown in Figure 7. Thermocouple tree 1 was at the right side of the compartment and was close to the initially ignited seat (see Figure 1(b)). The measured temperatures at 2.3 m high gradually increased to 155°C at 75 s, and then rapidly increased to 650°C at 106 s.

A quasi-steady state temperature of around 880°C was achieved after 135 s at 2.3 m above the floor within the experiment. The curve of predicted temperatures at this height essentially follows the measured trends but is shifted to the left by approximately 25 s. The measured temperatures at 1.0 m high increased slowly to 75°C at 100 s and 236°C at 171 s followed by a rapid increase due to the occurrence of flashover. The simulation has successfully reproduced the sudden change of the measured temperatures at this position.

After 200 s, temperatures at positions 1.0 m and 2.3 m above the floor become almost uniform. The predicted temperatures at 2.3 m above the floor are in good agreement with the measured data. However, the predicted temperatures at 1.0 m above the floor are higher than the measured values by approximately 200°C. It is seen from Figure 6(d) that the side walls and the carpet are all involved in fire at 180 s. From the predicted distribution of oxygen concentration and temperature at 210 s (Figure 8), it is known that the fire is already ventilation controlled and the thermocouple at a height of 1.0 m is within the hot layer. As the EDM represents a fast one-step reaction, the plume temperatures under a fuel rich situation are over-predicted compared with the measurements. As seen in Figure 8(b), the thermocouple at a height of 1.0 m is in the region with predicted temperatures over 1080°C.

Thermocouple tree 2 was on the left side of the compartment and opposite the initially ignited seat. Thermocouple tree 3 was near the doorway of the compartment. The measured temperatures at these two thermocouple trees have almost the same pattern of temperature changes as thermocouple tree 1. The model predictions of temperatures at these two thermocouples trees also follow the measured trends. As found at thermocouple tree 1, the temperature at 1.0 m above the floor at thermocouple tree 2 are also over-predicted. In contrast to these over-predictions, the predicted temperature at 1.0 m above the floor at thermocouple tree 3 is in good agreement with the measured data.

Finally, the heat fluxes measured by the two radiation detectors are compared with the model predictions in Figure 9. The positions of the two detectors are shown in Figure 1(b). Detector 1 was facing to the right and at 0.47 m above the

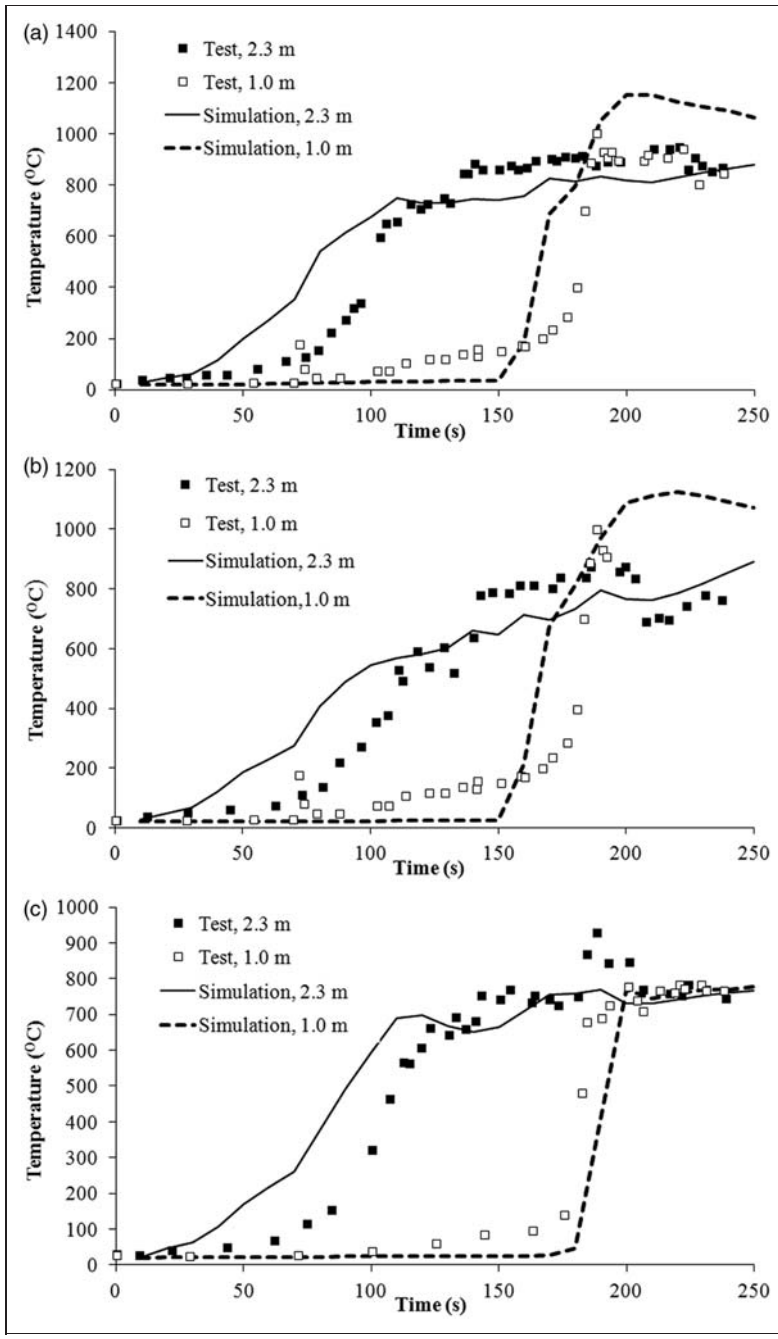

Figure 7. Measured and predicted temperatures at thermocouples at 2.3 m and 1.0 m above the floor of (a) tree 1, (b) tree 2 and (c) tree 3.

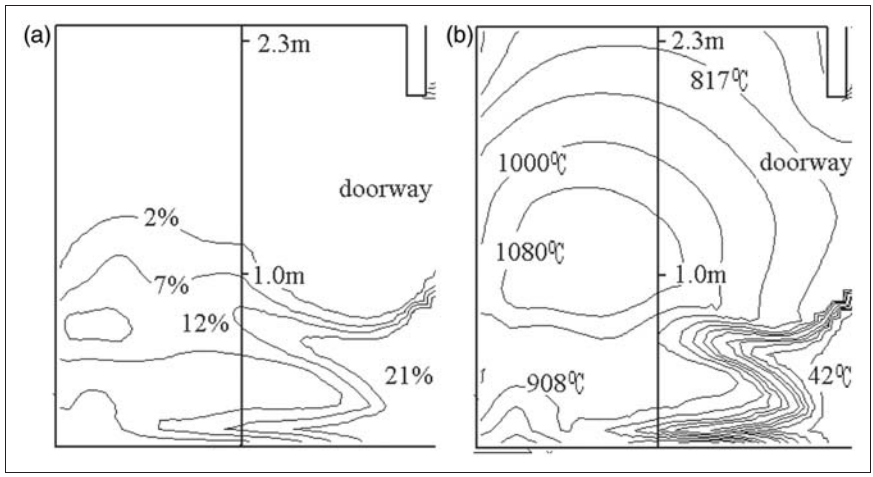

Figure 8. Predicted (a) oxygen concentration and (b) temperatures in a vertical plane passing through thermocouple tree 1 (vertical line) and the doorway at 210 s.

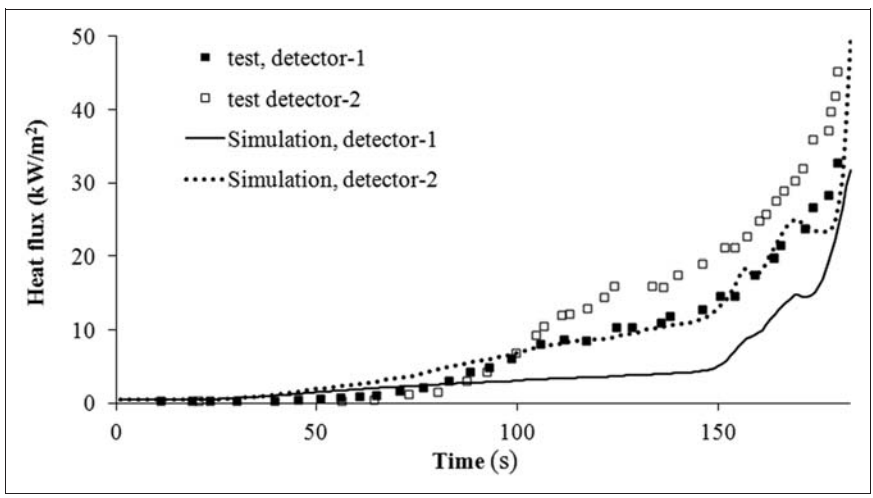

Figure 9. Measured and predicted radiation fluxes.

floor while detector 2 was facing upwards and at 0.48 m above the floor. The measured heat fluxes at the two locations were close to the ambient value of $0.4\,kW/m^2$ in the first 60 s and increased at almost an identical rate before 105 s. Differences between the measured heat fluxes at the two different locations appeared after this time. After flashover at 180 s, the measured heat fluxes at the two locations increased rapidly.

Although the predicted heat fluxes between 100 s and 180 s are lower than the measurements by relative errors up to 65%, the quantitative order between the two heat fluxes are preserved by the predictions. Since the heat fluxes are dependent not only on location but also the normal direction of the detector surface, it is difficult to produce the measured results with a high accuracy in the simulation.

Ignition criteria

In contrast to the conventional flame spread model with surface ignition temperature being the sole ignition criterion, an important feature of the flame spread model used in this study is the multi-ignition criteria. The advantage of using two ignition criteria is highlighted by comparing the above simulation results with those based solely on the surface ignition temperature. The scenario for these calculations, described in the preceding sections, is called the Base Case here.

The Base Case is repeated by simply switching off ignition criterion (b). In the first such calculation with criterion (b) off, the original burner of 7 kW remains as the ignition source. In this case, the fire self extinguishes after the burner is removed at 76 s. For the second calculation with criterion (b) off, following the procedure used for the Station Nightclub fire [15], an additional parameter is introduced into the model – an artificial initial HRR of 1500 kW/m^2 to start the combustion process. When this procedure is employed, it results in a predicted time to flashover of 46 s, which is much earlier than the 180 s observed in the test. A number of additional simulations were then performed in order to determine the optimal value of HRR for the ignition source so that a close match could be achieved between the observed and predicted onset of flashover. However, it was found that the predicted onset of flashover is extremely sensitive to the ignition source and so it was not possible to determine an optimal artificially inflated initial HRR.

Surface ignition temperature was also the only ignition criterion in the simulations performed in [1], which utilized the FDS code [14] with the same material properties as in the Base Case in this study. However, the model used in [1] did not use the flame spread rate parameter. Results from two of the simulations in [1] with mesh sizes similar to those used in this study are depicted in Figure 10. As seen in Figure 10(a), the predicted HRRs were very sensitive to the mesh density. Surprisingly, the finer mesh failed to produce better predictions of HRRs. While the coarser mesh predicted HRRs closer to the measured values, the simulation failed to reproduce the gradual increase of HRRs between 90 and 150 s, which results in the predicted temperatures at a height of 2.3 m at the three thermocouple trees (Figure 10(b)) being much lower than those both found in the experimental data and the predictions from the Base Case (Figure 7).

The discussion above has highlighted the deficiency in the use of surface ignition temperature as the sole ignition criterion in engineering applications of fire field models where flame spread over solid surfaces must be simulated. Using such an approach either causes uncertainty in using an adequate ignition source to create

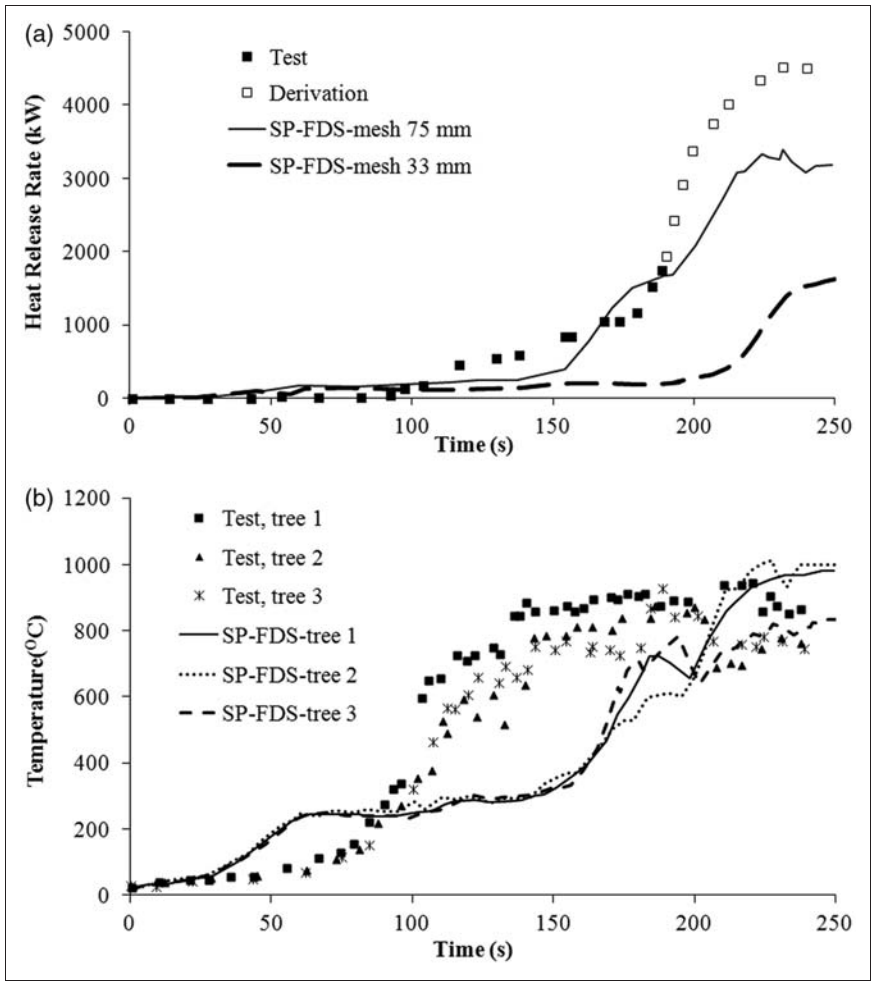

Figure 10. Predicted (a) heat release rate (HRRs) and (b) temperatures at 2.3 m above the floor in [1].

sustained flame spread or makes simulations very sensitive to mesh density. These two deficiencies are highly undesirable in producing consistent simulation results.

Uncertainty analysis

As there are uncertainties in the measured material properties used in the current study, it is necessary to quantify the effect of the uncertainty in the model inputs on the simulation results. The main burnable interior materials in rail car compartments usually include seats, wall panels, luggage racks, carpets etc. In the

experimental study, it was observed that the fire started from a seat base, spread to the seat back, the wall adjacent to the ignited seat and then burnt the overhead luggage racks [1]. The carpet was ignited only after the onset of flashover. Therefore, only the effect of the uncertainty in the input data for seats, wall panels and the wood racks and tables are analyzed.

As the cone calorimeter data and the flame spread rates of the train interior materials are the main model inputs in the current fire simulations, the effects of uncertainty in these data are analyzed in this section. Apart from the flame spread rates, all other data used in this study are the same as those used in [1], where relevant uncertainties were not reported. In a general investigation of the uncertainty of cone calorimeter data, it has been found that the estimated relative uncertainties in measured HRR from cone calorimeter tests are approximately 20–30% for 1 kW fires, 10% for 3 kW fires and less than 10% for 5 kW fires [22]. The HRRs of seats and wood from cone calorimeter tests (see Figure 3) are within the range of 1–3 kW. Therefore, an uncertainty of 15% is assumed for the HRR data for seats and wood. Since the HRR for HPL laminate is equivalent to a fire just above 1 kW but well below 1 kW for metal laminate, an uncertainty of 30% is assumed for these laminate HRRs. The same uncertainty values as those for HRR data are also assumed for the ignition temperature of each material.

The effect of the uncertainty of the input data on the simulation results is investigated in terms of the predicted time to flashover. It is noted from Table 3 that changes to the material properties of the seat materials have the most significant impact on the time to flashover while changes to the material properties of the metal laminate are the least significant. An uncertainty of 15% for the seat HRR or ignition temperatures results in a relative change of 36%–50% in the predicted time to flashover. A change of 30% in HRR or ignition temperature for the Metal laminate only leads to a less than 6% change of time to flashover. It is also noted that the changes in the predicted time to flashover caused by the under-estimation of HRR or over-estimation of the ignition temperature (46%–50%) are larger than those caused by the over-estimation of HRR or under-estimation of the ignition temperature (12%–39%) except for the metal laminate.

The uncertainty caused by the flame spread rate is analyzed for the seat only as the wall panels are ignited after 60 s (see Figure 6), at which time a hot upper layer has formed. Once a hot layer has formed, the effect of the ignition criterion (b), i.e. the flame spread rate, can be ignored. The flame spread rates used in this study are estimated based on the images of burning double seats provided in the experimental report. If this estimation has an error of $\pm 15\%$ for the upward rate, the lateral rate and the downward rate, the changes in the predicted time to flashover will be within the same magnitude, -12% and $+18\%$, respectively.

The results of the uncertainty analysis listed in Table 3 can be used to assist in selecting compartment interior materials in terms of fire safety. For example, most common train fires are the result of arson, which account for around 56%–68% of total train fires [23,24]. Arson fires often start on the top of seats or in a corner of the car.

Table 3. Sensitivities of predicted times to flashover to uncertainties in material properties

Material	Uncertainty	Predicted time to flashover (s)	Relative changes (%) compared with 165 s in Base Case
PUR seat	+15% for HRR	106	–36
	–15% for HRR	247	+50
	+15% for ignition temperature	244	+48
	–15% for ignition temperature	100	–39
	+15% for flame spread of seat	145	–12
	–15% for flame spread of seat	195	+18
Metal laminate wall panel	+30% for HRR	165	0
	–30% for HRR	165	0
	+30% for ignition temperature	165	0
	–30% for ignition temperature	155	–6
HPL laminate wall panel	+30% for HRR	127	–23
	–30% for HRR	242	+47
	+30% for ignition temperature	248	+50
	–30% for ignition temperature	142	–14
Wood tables and racks	+15% for HRR	138	–16
	–15% for HRR	242	+47
	+15% for ignition temperature	241	+46
	–15% for ignition temperature	126	–24

Consequently, the flammability properties of seats are of significant importance in determining the early stages of train fire development. Therefore, it is important in terms of fire safety to select adequate seat materials for trains. The reported ignition temperatures for rail car seats vary within a wide range, 346°C in the experiment in [1] and 448°C in Singapore Circle Line stock [25]. As seen in Table 3, an increase of ignition temperature of 15% for seats can delay the time to flashover by 48%.

Effect of porosity of overhead rack structure

In the fire experiment in [1], there were holes in the overhead luggage rack structure (Figure 1). In reality, luggage racks vary considerably in configuration, from thin plates without openings to configurations with many small holes or other types of openings. The effects of rack openings or porosity on fire development can be demonstrated using two extreme scenarios. On one hand, hot gases may

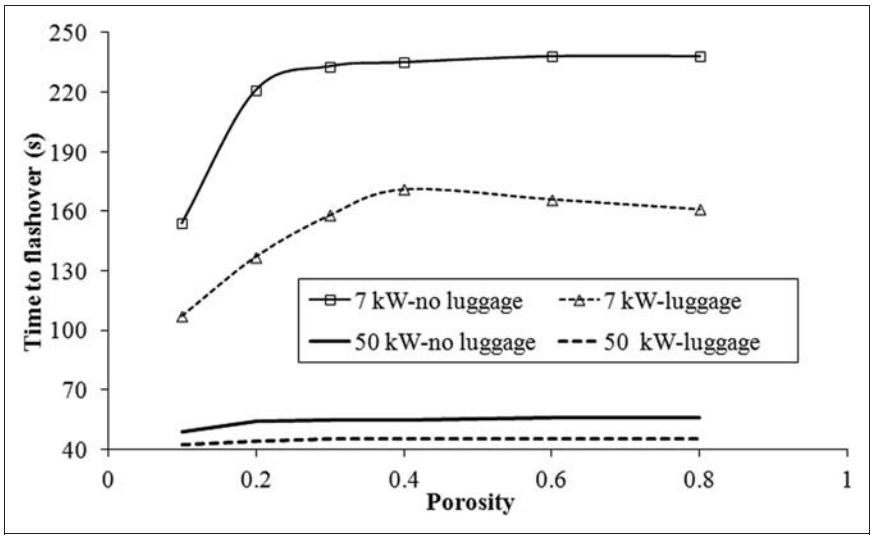

Figure 11. Predicted time to flashover as a function of luggage rack porosity.

accumulate in the space between the seats and the racks if the porosity of the racks is low or there are no openings in the rack, facilitating the creation of ceiling jets under the racks. In the other extreme, hot gases may readily pass through the rack if it has large openings and accumulate under the ceiling of the railcar. These factors can assist compartment fire development either through rapid flame spread along the seats in the first case or through ignition of the luggage or the upper part of the wall panels in the second case. In this section, the effects of porosity within the luggage rack on time to flashover are investigated with the assumption that the racks are non-combustible.

Two luggage scenarios, L1 and L2, are considered in this study. In L1, there is no baggage on the luggage racks. In L2, there is a small carry-on bag on the luggage rack, which is placed directly above the initially ignited seat. The bag is assumed to have dimensions of 0.4 m × 0.4 m and is 0.2 m thick. The properties of the bag are assumed to be the same as the PUR foam used in seats (see Table 1). However, the HRRPUA is derived from the burning rate of a trash bag in [25] and shown in Figure 3. For arson fires, the size of the ignition source varies between several kW and hundreds of kW. To investigate the dependence of time to flashover on the size of the ignition source with various porosity levels of the luggage racks, two ignition source scenarios, I1 and I2, are considered. Scenario I1 consists of a 7 kW fire ignition source used in the experimental study in [1] while I2 consists of a large ignition source of 50 kW.

In total, 24 fire scenarios were run as part of this analysis.

Figure 11 depicts the time to flashover as a function of the porosity level of the luggage rack with the two different ignition sources. With the small ignition source (7 kW), the predicted time to flashover in the scenario L1 (no luggage) quickly

increases from 154 s to 221 s with the change of rack porosity from 0.1 to 0.2. However, the predicted time to flashover remains almost constant when the porosity of the racks is greater than 0.3. The maximum time to flashover is 238 s with porosities of 0.6–0.8. When a small bag is put on the rack and directly above the fire source, the predicted time to flashover increases with the increase of the porosity of the racks until the porosity level reaches 0.4. Afterwards, the time to flashover declines with the increase of the porosity of the racks, but the change of time to flashover is quite small. Furthermore, for a given porosity value, the case with luggage is significantly faster than the case without luggage, occurring on average 32% earlier.

With a large ignition source (50 kW), the effect of the porosity on the time to flashover still follows the same trends as observed with the small ignition source. However, due to the fast development of the fire, the observed dependency of time to flashover on porosity and the presence of luggage is small. Indeed, the impact of rack porosity can be neglected altogether.

For a small ignition source, the porosity level of the luggage rack can be quite influential, significantly delaying the time to flashover. However, once the porosity reaches a certain level, the time to flashover is no longer influenced by the porosity value.

Conclusions

A fire test within a small rail car compartment has been reproduced using an enhanced flame spread model. The flame spread model utilizes two ignition criteria – ignition temperature and flame spread rate – compared to the conventional single ignition criterion model which only makes use of the surface ignition temperature. From the analysis of these simulations it is found that

- The enhanced flame spread model has a significant advantage over the conventional flame spread model in that it is significantly less sensitive to the computational mesh and does not need an arbitrarily assumed value of heat release rate of the ignition source;
- The enhanced model is capable of reproducing the fire test results, in particular:
  - The predicted burning locations are in line with the experimental observations during the entire test;
  - The predicted HRRs are in good agreement with measurements;
  - The predicted time to flashover (165 s) is within 9% of the experimental result (180 s);
  - The predicted temperatures at both heights (2.3 m and 1.0 m above the floor) for all three thermocouple trees essentially follow the measured trends;
  - The predicted heat fluxes at the locations of the two radiation detectors in the test essentially follow the measured trends.
- For the materials examined in this study (PUR seat materials, metal laminate wall panels, HPL laminate wall panels and wood tables) the uncertainties in

specifying material properties will impact the predicted time to flashover, in particular:
  - With the exception of the metal laminate, under-estimating the HRR or over-estimating the ignition temperate by 15% to 30% can increase the time to flashover by between 46% and 50%.
  - With the exception of the metal laminate, over-estimating the HRR or under-estimating the ignition temperate by 15% to 30% can decrease the time to flashover by between 14% and 39%.
  - The time to flashover is most strongly dependent on variations in seat material properties, with changes in time to flashover of up to 50% being observed for changes in HRR or ignition temperature of 15%.
  - The time to flashover is least dependent on variations in the material properties of the metal laminate, with changes in time to flashover of up to 6% being observed for changes in HRR or ignition temperature of up to 30%.
  - Uncertainties of $\pm 15\%$ in the estimated flame spread rates for seats produce similar relative changes in the time to flashover (-12% and $+18\%$).
  - These results are only relevant to the scenarios investigated in this study, i.e., within a small rail car compartment and using a small ignition source.
- For a small ignition source, the porosity level of the luggage rack can have a significant impact on fire development. As the porosity level increases, the time to flashover is delayed. However, once the rack porosity reaches a critical level, the fire development is no longer influenced by the porosity level. For large ignition sources, the fire development is not significantly affected by the porosity level.

The flame spread model presented in this study makes use of flame spread rates as a model parameter. Flame spread rates can be measured or estimated from specific apparatus designed for measuring such rates or from material burning tests. However, it may be difficult experimentally to generate similar conditions (relating to heat flux and geometry) to those required by a specific modeling application. Alternatively, flame spread rates can be calculated from numerical tests using more fundamental flame spread models involving pyrolysis mechanisms.

Acknowledgments

Ms Hu would like to thank FSEG of the University of Greenwich for their financial support through the PhD Bursary Program. The authors would like to thank Ms Maria Hjohlman of SP Technical Research Institute of Sweden for kindly providing unpublished details regarding the fire test used in this study.

Funding

This research received no specific grant from any funding agency in the public, commercial, or not-for-profit sectors.

References

1. Hjohlman M, Försth M and Axelsson J. *Design fire for a train compartment*, SP Report 2009:08; Fire Technology, Boras, Sweden, SP Technical Research Institute of Sweden, 2009.
2. Peacock RD and Braum Emil. *Fire safety of passenger trains; Phase I: Material Evaluation (Cone Calorimeter)*, NISTIR 6132, National Institute of Standards and Technology, Gaithersburg, MD, USA, 1999.
3. Peacock RD, Averill JD, Madrzykowski D, et al. *Fire safety of passenger trains; Phase III: evaluation of fire hazard analysis using full-Scale passenger rail car tests*, NISTIR 6563, National Institute of Standards and Technology, Gaithersburg, MD, USA, 2004.
4. Ingason H. Model scale railcar fire tests. *Fire Saf J* 2007; Vol. 42: 271–282.
5. White N, Dowling V and Barnett J. Full-scale fire experiment on a typical passenger train. In: *Fire safety science-proceedings of the eighth international Symposium*, International Association for Fire Safety Science, London, 2005, pp.1157–1168.
6. Ewer J, Grandison A, Jia F, et al. *User Guide and Technical Manual, SMARTFIRE V4.1*, Fire Safety Engineering Group, The University of Greenwich, London, 2007.
7. Jia F, Patel MK, Galea ER, et al. CFD Fire Simulation of the Swissair Flight 111 In-flight fire – Part II: Fire spread within the simulated area. *Aeronaut J Royal Aeronaut Soc* 2006; Vol. 11: 303–314.
8. Wang Z, Galea ER and Jia F. A CFD simulation of a post-crash aircraft fire test. *J Aircraft* 2012.
9. Galea ER, Wang Z, Veeraswamy A, et al. Coupled fire/evacuation analysis of station nightclub fire. In: *Fire Safety Science-proceedings of the ninth international Symposium, International Association for Fire Safety Science*, London, 2008, pp.465–476.
10. Galea ER, Filippidis L, Wang Z, et al. Fire and evacuation analysis in BWB aircraft configurations: computer simulations and large-scale evacuation experiment. *Aeronaut J Royal Aeronaut Soc* 2010; Vol. 114: 271–277.
11. Galea ER. On the field modeling approach to the simulation of enclosure fires. *J of Fire Protection Eng* 1989; Vol. 1: 11–22.
12. Cox G (ed.) *Combustion fundamentals of fire*. London: Academic Press, 1995.
13. Magnussen BF and Hjertager BH. On mathematical modeling of turbulent combustion with special emphasis on soot formation and combustion. In: *16th Symp. (Int) on Combustion*, the Combustion Institute, Pittsburgh, 1977.
14. McGrattan K, Klein B, Hostikka S, et al. *Fire dynamics simulator (version 5) user's guide*. Gaithersburg, MD: National Institute of Standards and Technology, 2007.
15. Grosshandler W, Bryner N, Madrzykowski D, et al. *Report of the technical investigation of the station nightclub fire*. NIST NCSTAR 2: Vol. I-II. Gaithersburg, MD: National Institute of Standards and Technology, 2005.
16. Babrauskas V. *Ignition handbook*. Issaquah, WA: Fire Science Publishers, 2003.
17. Hasemi Y. Surface flame spread. *The SFPE handbook of fire protection engineering*, 4th ed. Quincy, MA: National Fire Protection Association, 2008, pp.2.278–2.290.
18. Qian J. Prediction of LIFT data from cone calorimeter measurement. In: Barauskas V, SJ Grayson E, Spon FN (eds) *Heat release in fires*. London: E & FN Spon, 1995.
19. Tewarson A. Generation of heat and chemical compounds in fires. *The SFPE handbook of fire protection engineering*, 2nd ed. Quincy, MA: National Fire Protection Association, 1995, pp.3.53–3.124.
20. Drysdale Dougal. *An introduction to fire dynamics*. Chichester: Wiley, 1985.

21. Peacock D, Reneke PA, Bukoski RW, et al. Definition of flashover for fire hazard calculation. *Fire Saf J* 1999; Vol. 32: 331–345.
22. Zhao L and Dembsey N. Measurement uncertainty analysis for calorimetry apparatuses. *Fire Mater* 2008; Vol. 32: 1–26.
23. Chiam BH. *Numerical simulation of a metro train fire*. Fire Engineering Research Report 05/01, Department of Civil Engineering, University of Canterbury, New Zealand, 2005, p.340.
24. Hudson S. *Train Fires – Special Topic Report*, Railway Safety, UK, RSSB, January, 2001.
25. Peacock RD, Reneke PA, Averill JD, et al. *Fire safety of passenger trains; Phase II: Application of fire hazards analysis techniques*, NISTIR 6525, National Institute of Standards and Technology, Gaithersburg, MD, USA, 2002.